Winter 12-2017

Light Dynamics in the Damariscotta River Estuary With Implications for Microphytobenthos

Teiga C. Martin
University of Maine

LIGHT DYNAMICS IN THE DAMARISCOTTA RIVER ESTUARY WITH IMPLICATIONS FOR MICROPHYTOBENTHOS

by

Teiga C. Martin

A Thesis Submitted in Partial Fulfillment
of the Requirements for a Degree with Honors
(Marine Science)

The Honors College
University of Maine
December 2017

Advisory Committee:

Damian C. Brady, Assistant Professor, School of Marine Sciences
Larry Mayer, Agatha B. Darling Professor of Oceanography
Emmanuel Boss, Professor, School of Marine Sciences
Jeremy Rich, Assistant Professor, School of Marine Sciences
Mark Haggerty, Rezendes Preceptor for Civic Engagement, Honors College

ABSTRACT

Predicting benthic light fields in the Damariscotta River Estuary (DRE) allows us to evaluate optimal microphytobenthos habitat, and determine the most the productive regions of the DRE. A model was created using instantaneous photosynthetically active radiation (PAR) to predict the spatial distribution of sufficient light fields for primary production along the benthos of the estuary. PAR was collected at six stations oriented N-S along the DRE during late September in 2016 and 2017. Calculated at each station was $Z_{1\%}$, experimental and model diffuse coefficients of light (K_d), and the optimal light level depth for microphytobenthos production. Light fields were extrapolated between stations over bathymetric data of the DRE. Optimal light fields for microphytobenthos primary production are present along the edges of the entire DRE, and above 43.91º N. Light only reaches the benthos at the head of the estuary, and more light penetrated the water column in 2017. Light attenuates as a function of the concentration of scattering and absorbing agents, and spectral quality has a direct relationship with depth.

TABLE OF CONTENTS

LIST OF TABLES AND FIGURES

INTRODUCTION

Phytoplankton primary production, a light driven process, accounts for nearly 50% of global primary production, and drives the planktonic and microbial food web below the euphotic zone (Liu 2005). The euphotic zone defines the region where photosynthesis occurs. Spectral light quality decreases through the water column as a function of absorption and scattering by dissolved- and suspended particulate matter (Liu 2005). Primary production occurs at the surface, within the water column, and at the benthos (bottom) of marine systems.

Phytoplankton are a vital component of aquatic ecosystems. Productivity in littoral regions (where sunlight reaches the benthos) of lakes and coastal waters outweighs productivity in open oceans because of the diversity of mirco- and macroalgae primary producers. Primary producers are the base of the food chain, and phytoplankton are a critical component of trophodynamics; their biomass supports a diversity of species in higher trophic levels, ranging from microorganisms and benthic invertebrates, to pelagic fishes and sea birds. Plankton globally populate the neritic zone, the region extending from the pelagic zone to the benthos before the abyssal drop-off.

Understanding benthic light fields is important because benthic primary production contributes to total primary production (Cahoon 1993). The contribution of benthic production to global production is unknown, however, because benthic environments are diverse, and benthic light fields remain largely unstudied. The majority of research on benthic primary production is localized to regions in North America and Europe, leaving arctic and tropical regions largely unstudied (Gattuso *et al*. 2006).

One of the primary contributors to benthic primary production are benthic microalgae, termed "microphytobenthos." Microphytobenthos are "microscopic, unicellular eukaryotic algae (Baccilariophyceae, Chlorophyceae and Dinophyceae) and the prokaryotic Cyanobacteria" (Aberle-Malzahn 2004). Microphytobenthos form thin, brown-green mats primarily composed of diatoms (Admiraal 1984). In temperate latitudes, mats are seasonally populated by Cyanobacteria, coccal and filamentous green algae (Nozaki *et al*. 2003; Yallop *et al*. 1994). Benthic diatoms are mostly pennate and prostrate in form, with epipelic or epipsammic lifestyles, where they grow on muddy or sandy sediments, respectively. Microphytobenthos can be found on sediment surfaces in a variety of ecosystems, ranging from subtidal sediments and salt marshes, to intertidal mud and sand flats (Mirbavkar and Anil 2002).

Microphytobenthos mats vary in structure across changing environments. Mats have more biomass in sheltered, muddy environments compared to exposed, sandy environments. Bottom-currents can break mats, suspending individuals into the water column (Delgado 1989), decreasing community biomass. Microphytobenthos mats are held together by mucilaginous films, which increase the critical sheer stress of the mats, and decrease the rate of resuspension (Delgado *et al.* 1991). Diatoms also excrete extracellular polymeric substances (EPS) at a rate directly proportional to their rate of productivity (Cadée and Hegemann 1974). In intertidal environments, diatoms increase EPS secretions prior to tidal immersion as they migrate vertically downwards in a short-term response to increased bottom-currents and light availability (Underwood and Smith 1998). Both mucilaginous films and EPS secretions secure mats. Not only is biomass controlled by the physical environment, it is also determined by primary production.

High rates of productivity correspond to greater mat biomass. The rate of primary production is proportional to light transmission through the water column. Light transmission is dependent on the amount of solar radiation reaching the water. Solar radiation reaching the water depends on sun angle, latitude, season, time of day, and cloud cover. When light hits the surface, it can either reflect away or refract into the body of water. Light that penetrates water is either scattered or absorbed by light attenuating agents. Light is primarily attenuated by absorbing agents, such as chromophoric dissolved organic material (CDOM). Scattering agents are water-column phytoplankton and suspended particulate material (SPM). Smaller particles scatter more light. The amount of light penetrating the water column is described by the light attenuation coefficient (K_d). Large K_d values indicate poor water quality with high concentrations of light attenuating agents, and low K_d values indicate clear water with low concentrations of light attenuating agents. Microphytobenthos are more productive in environments with low K_d values (Baker and Lavelle 1984).

Another proxy that can be used to determine phytoplankton productivity is the 1% light level ($Z_{1\%}$). $Z_{1\%}$ is a theoretical value that describes the floor of the euphotic zone, the region where primary production occurs. At $Z_{1\%}$, only 1% of solar radiation available at the surface is transmitted through the water column. $Z_{1\%}$ is also known as the compensation depth because rates of production and respiration are equal. Below $Z_{1\%}$, the rate of respiration is greater than the rate of productivity, and plankton consequently perish (Coljin 1982; Ryther and Menzel 1959). $Z_{1\%}$ is only a theoretical depth describing viable habitat; in reality, plankton are reliant on absolute light levels.

Absolute light is quantified as photosynthetically active radiation (PAR), the amount of photons available at depth between the practical range of solar radiation of 400 – 700nm for photosynthesis (Tyler 1966). PAR exponentially decreases with depth due to light attenuating agents. Absorbing agents are primarily responsible for PAR attenuation. (Kirk 1977). Longer wavelengths attenuate first (i.e. red wavelengths: 620-750nm), so the majority of the light resources available at depth are shorter wavelengths (i.e. blue and green wavelengths: 450-495nm and 495-570nm, respectively). Blue and green wavelengths can penetrate up to 75-100m in clear waters, while red wavelengths that attenuate within the first 5m (Kirk 1994). Primary producers can photosynthesize in reduced light conditions because they have special pigments that primarily absorb in the blue and green wavelengths. Chlorophyll a absorbs wavelengths maximally between 430 – 662nm, and chlorophyll b absorbs maximally between 453 – 642nm. Photosynthesizers also have accessory pigments, such as carotenoids, that absorb light between 460 – 550nm (Netto *et al.* 2005; Taylor *et al*. 2010).

Microphytobenthos have also adapted to variations in spectral light quality by using accessory pigments and photoreceptors to modify photophysiological responses based on the presence, absence, and ratios of available wavelengths (Ashworth *et al*. 2013; Falciatore and Bowler 2005). Cryptic blue light receptors, also known as "cryptochromes," are present in most terrestrial and marine photosynthetic organisms, including marine diatoms. Marine diatoms are the primary constituent of microphytobenthos mats, and cryptochromes help them absorb low-quality light at the benthos (Falciatore and Bowler 2005).

Although microphytobenthos are limited to a small habitat range where sufficient light reaches the benthos (Coljin 1982), they have adapted to maximize productivity rates. Similar to other primary producers in low-intensity light environments, microphytobenthos in subtidal regions have high concentrations of light harvesting pigment antennae. Light harvesting pigment antennae absorb low-intensity light and transfer it to reaction centers where it is converted into chemical energy, such as ATP and NADPH (Taylor *et al*. 2010). High concentrations of pigment antennae allow individuals to take advantage of ambient light resources. Furthermore, microphytobenthos populate the sediment-water interface because light only penetrates the upper 0.2 – 2.0mm of sediment. Light penetration into sediment varies as a factor of grain size and absorbing material in the benthos, such as algae and organic coatings on sediment. To avoid self-shading, mats are approximately only 1mm thick (Coljin 1982; MacIntyre *et al.* 2000).

Not only are microphytobenthos adapted to low-intensity light conditions in subtidal zones, they are also adapted to high-intensity light conditions in intertidal zones. During tidal emersion and summer solar maxima, intertidal ecosystems can be exposed to over 2000$\mu Em^{-2}s^{-1}$of solar energy, and temperatures can exceed 30ºC (Blanchard *et al*. 1996; Perkins *et al*. 2001). In stressful high-intensity light environments, photo-oxidative damage causes pigment bleaching, which leads to cellular death. The fastest response to increased solar radiation is nonphotochemical chlorophyll fluorescence quenching (NPQ). NPQ is a reversible process that protects microphytobenthos from photo-damage by thermally dissipating excess absorbed energy (Müller *et al.* 2001). Additionally, microphytobenthos can reduce the size of light harvesting pigment antennae, effectively adjusting light absorption through gene expression and proteolysis (Govindjee 2002).

Furthermore, microphytobenthos have photo-acclimated to "micro-migrate" into benthic sediments to escape photo-damage (Kromkamp *et al*. 1998).

In all environments, microphytobenthos demonstrate diel vertical migration. Individuals migrate at rates ranging between 10-27mmh^{-1} in response to changing physical properties, such as light availability, desiccation, tidal cycles, resuspension, and predation (de Jong and Admiraal 1984; Hopkins 1963; Perkins *et al.* 2001; Pinckney and Singmark 1991). Although nutrient concentrations quickly decrease in benthic sediments (Joergensen *et al*. 1983), microphytobenthos are only minimally impacted because they only descend a few millimeters (Admiraal 1977; Admiraal 1984).

Microphytobenthos partially control the flux of nutrients, such as nitrate, on the sediment-water interface. Microphytobenthos facilitate sediment denitrification, a microbially driven process that reduces nitrate and produces nitrogen gas via respiration (Zumft 1997). Similar to all organisms, microphytobenthos require many nutrients to grow and reproduce. Essential nutrients are carbon, nitrogen, phosphorus, oxygen, iron, zinc, copper, magnesium, potassium, silica, and calcium. Nitrogen and phosphorus are two of the most essential nutrients for aquatic photosynthesizers (NOAA 2008).

Freshwater runoff can become rich in nitrogen and phosphorus after passing over a variety of sources ranging from decomposing organic material, wildlife waste, and geologic formations saturated with nitrate or phosphate, to industrial wastewater, fertilized land, and sewage treatment plants. While organisms are reliant on sufficient concentrations of nitrogen and phosphorus, waters become polluted when concentrations exceed a threshold; thresholds are unique to each ecosystem. Excess nutrients instigate plankton blooms, which can deplete dissolved oxygen concentrations, and lead to eutrophication. Eutrophic environments have

critical dissolved oxygen (DO) concentrations, negatively impacting respiring organisms. In extreme cases, eutrophication can lead to hypoxic (very low oxygen) and anoxic (no oxygen) conditions (NOAA 2008; Taylor *et al.* 2010).

Plankton blooms persist until excess nutrients are consumed. During blooms, primary production rates and biomass can increase over several orders of magnitude. Microphytobenthos bloom during the winter and early spring when there are excess nutrients, and when solar radiation is maximal. While blooming, microphytobenthos assimilate nutrients from the water column, reducing pelagic inorganic nitrogen and phosphorus. By incorporating excess nutrients from the water column, microphytobenthos help mitigate potential or current eutrophic conditions. Mats also act as benthic armoring, reducing sediment suspension and scattering agents (Cerco and Seitzinger 1997; Orth and Moore 1983; Sundbäck *et al.* 2000; Underwood and Kromkamp 1999).

Microphytobenthos blooms have an inverse relationship with water-column phytoplankton blooms. Water-column phytoplankton bloom in the late spring and early summer. While blooming, water-column phytoplankton attenuate light, shading microphytobenthos. Resultantly, microphytobenthos productivity and biomass decline, decreasing the rate at which they assimilate nutrients from the water column (Underwood and Kromkamp 1999). Following plankton blooms, DO concentrations decrease due to planktonic decomposition. Decomposing phytoplankton biomass is transported horizontally across estuaries from tidally driven currents, extensively reducing DO concentrations. Conversely, decomposing microphytobenthos biomass remains at the benthos, only locally reducing DO concentrations. Resultantly, phytoplankton decomposition has greater negative impacts on higher trophic levels than microphytobenthos decomposition.

The Study System

The Damariscotta River extends 30.6km in northeast-southwest orientation, beginning at the freshwater outlet of Damariscotta Lake in Damariscotta Mills, Maine, and emptying into the Gulf of Maine near Pemaquid Point in Bristol, Maine (GNIS Detail). The river is fed by tributaries from the north, originating in Somerville and Washington, and extending 19km north into Jefferson. The tidewater begins at Salt Bay, a junction 15m below Damariscotta Lake in elevation (GNIS Detail). The Damariscotta River Estuary (DRE) begins where fresh and salt waters mix at Salt Bay, and flows southward through several towns (Newcastle, Edgecomb, Boothbay, Damariscotta, Bristol, and South Bristol) before reaching the Atlantic Ocean (Hayward 2010).

The DRE is a tidally driven drowned river valley. Although partially stratified near the head, it is well-mixed near the mouth as the benthic topography generally declines. Mixing along the DRE occurs where the width of the estuary drastically narrows, such as at Fort Island and Fitch Point (Glidden Ledges). Mixing is physically and ecologically important because it increases homogeneity within the estuary. South of Fort Island, the DRE ends and becomes predominantly seawater (McAlice 1977).

The DRE is economically important to surrounding towns because of the revenue drawn from tourism, fishing, clamming, marine worming, and aquaculture (DMR Aquaculture Division 2017). The DRE is the most productive aquaculture center in Maine, home to eight commercial farms: Dodge Cove Marine Farm, LLC; Glidden Point Oyster Co.; Johns River Shellfish, LLC; Maine Fresh Sea Farms, LLC; Mook Sea Farms, Inc.; Muscongus Bay Aquaculture, Inc.; Norumbega Oyster, Inc.; and Pemaquid Oyster Company, Inc. (DMR Aquaculture Division 2017).

In Maine, oyster aquaculture is over a $5 million industry, and a large portion of production occurs in the DRE. Populating both the surface waters and benthos of the estuary are oyster rafts from seven of the eight aquaculture farms listed above, only excluding Maine Fresh Sea Farms, LLC, which specializes in marine alga (DMR Aquaculture Division 2017).

Modeling benthic light fields in the DRE helps spatially predict optimal microphytobenthos habitats. As ecologically and trophically important primary producers, microphytobenthos communities positively impact estuarine systems by facilitating nutrient cycling, and providing a rich food source for naturally occurring and for cultured organisms.

MATERIALS AND METHODS

Estuarine Oceanography Cruise Data

Two oceanographic research cruises were conducted on 21 September 2016 and on 27 September 2017 on the R/V *Ira C*. At six stations along the DRE, a SeaBird EcoSampler CTD (conductivity, temperature, depth) rosette was deployed, and a SeaBird Scientific PAR sensor recorded PAR from the surface to depth. GPS coordinates were recorded for each station. Depth was determined using the CTD. Station 1 is located at the mouth, and Station 6 is located at the head of the DRE.

MATLAB

The optical data used in this model is presented in tables 1 and 2. The model uses instantaneous PAR (PAR measured at a particular instance, not averaged over a time period) to calculate Io (solar irradiance at one meter below the surface) and Iz (solar irradiance at depth). The light attenuation coefficient, $K_d = -[\log(Iz/Io)]/Z$. K_d is derived from the equation: $Iz=Io*e^{(-K_d*Z)}$, where Z = depth. K_d values were used to determine where optimal light fields ($I>90\mu Em^{-2}s^{-1}$) (Cerco and Seitzinger 1997) are present along the DRE. Irradiance and K_d values were related to bathymetry at each station, then extrapolated between stations to generate light fields along the entire DRE (bathymetric data of the DRE was generated by Katie Coupland).

Theoretically, at $Z_{1\%}$, only 1% of Io is transmitted through the water-column, so $Iz=0.01(Io)$. $Z_{1\%}$ was calculated using the Lambert-Beer Law: $Z_{1\%}=\ln(0.01)/(-K_d)$. Model K_d values were calculated with the assumption that $Iz=0.01(Io)$. Bottom-weighted K_{dw}

plots were generated with a linear model that weights K_{dw} values along the benthos at each station. Bottom-weighted K_{dw} values emphasize benthic light fields.

Compared against plots of insolation reaching the benthos are: 1) the model semilog(x) of K_d reaching the benthos, with the assumption that Iz = 0.01(Io); 2) non-weighted K_d residuals reaching the benthos; and 3) bottom-weighted K_d residuals reaching the benthos.

Several assumptions were made while generating the model: 1) uniform microphytobenthos mat thickness and species composition; 2) PAR attenuation is exponential with depth (Kirk 1977); 3) uniform light resources; 4) uniform microphytobenthos photosynthetic efficiency; 5) uniform daylight spectral composition; 6) uniform turbidity; 7) no nutrient limitations; 8) no grazing, suspension, or other disturbance events.

RESULTS

DRE depth increases from the head (Station 6) to the mouth (Station 1) of the DRE, with the exception of Station 5 where the depth slightly increases (Tables 1 and 2). $Z_{1\%}$ increases from the head to the mouth of the DRE at all stations in 2016, and increases from the head to the mouth in 2017, with the exception of Station 5 (Tables 1 and 2). In 2016 at Station 3 (Glidden Ledges) bottom depth decreases drastically, then increases again in Station 2; conversely, $Z_{1\%}$ increases at Station 3, then decreases at Station 2 (Table 1).

In 2016, experimental K_d values decrease from the head to the mouth of the DRE, except for a spike at Station 4. Model K_{dw} values decrease from the head to the mouth of the DRE, except for spikes at Stations 3 and 5. Experimental K_d values are larger than model K_{dw} values, except at Stations 2 and 5 (Table 1).

In 2017, experimental K_d values increase from Station 6 to Station 5, then decreases toward the mouth of the DRE. Model K_{dw} values also increase from Station 6 to Station 5, then decreases toward the mouth of the river, except for a spike at Station 4. Experimental K_d values are less than model K_{dw} values, except at Station 3 where they are equivalent, and at Station 5 where experimental K_d is greater (Table 2). 2016 K_d values were consistently greater than 2017 values (Tables 1 and 2).

PAR and irradiance attenuate exponentially with depth (Figs. 1 – 14). In 2016 and 2017, PAR reaches the benthos in Stations 5 and 6, but attenuates to “zero” (a level undetectable by the sensor) before reaching the benthos in Stations 1 – 4 (Figs. 1 and 2). In 2016, irradiance at Glidden Ledges drastically decreases near the benthos, and the exponential assumption predicts a greater value than ambient light levels (Fig. 6).

In 2016, at Stations 1 and 6, non-weighted residual profiles indicate less irradiance at the surface than at the benthos, while bottom-weighted profiles indicate more irradiance at the surface than at the benthos (Figs. 3 and 8). Light attenuation is therefore stronger at depth than near the surface due to non-homogeneous vertical distribution of material. At Stations 2 – 5, non-weighted residuals indicate less benthic irradiance, while bottom-weighted profiles indicate more benthic irradiance (Figs. 4 – 7). Stations 4 – 6 have a spike decrease in light attenuating agents at 0.5m, and a spike increase at 1m (Figs. 3 – 5).

In 2017 at Stations 3 – 6, non-weighted residual profiles indicate less irradiance at the surface than at the benthos, while bottom-weighted profiles indicate more irradiance at the surface than at the benthos (Figs. 10 – 12). At Station 2, non-weighted residuals indicate less benthic irradiance, while bottom-weighted profiles indicate more benthic irradiance (Fig. 13). At Station 1, irradiance in both the non-weighted and the bottom-weighted profiles attenuates to "zero" (Fig. 14). Furthermore, K_{dw} values negatively spike at 15m in the bottom-weighted profile, but not in the non-weighed or irradiance plots, indicating a flaw in the model, not increased light attenuating agents (Fig. 14).

Irradiance has a positive relationship with bottom-depth and latitude. The greatest amount of light reaches the benthos along the edges of the DRE above 43.91ºN (Figs. 15 – 18). Above 43.91ºN, and on the edges of the estuary, $I>90\mu Em^{-2}s^{-1}$ at the benthos (Figs. 17 – 18). Irradiance values never drop below $90\mu Em^{-2}s^{-1}$ at Stations 5 and 6 in 2016 and in 2017 (Tables 1 and 2). In 2016, irradiance is consistently less than $90\mu Em^{-2}s^{-1}$ at depths below 23m at Stations 1 – 4 in 2016 (Table 1). In 2017, $I<90\mu Em^{-2}s^{-1}$ below 10m at Stations 3 and 4, below 11.5m at Station 2, and below 12.75m at Station 1 (Table 2).

DISCUSSION

Physical Drivers

This model provides a basic illustration of benthic light fields in the DRE by calculating K_d from depth profiles of instantaneous PAR, and calculating depths where the half saturation value ($I=90\mu Em^{-2}s^{-1}$) occurs. The model efficiently generates light profiles that closely match instantaneous irradiance values.

In locations with unique benthic topography, such as Glidden Ledges (Figs. 6, 12), turbidity increases from enhanced water circulation and bottom currents. Increased turbidity is likely attributed to benthic sediment suspension. It is suspected that there is reduced microphytobenthos biomass at Glidden Ledges due to the higher likelihood of suspension and decreased light availability, although there are no observations supporting this hypothesis.

The DRE was more turbid in 2016 than in 2017 (Tables 1 and 2). Interestingly, 2016 experienced much lower annual rainfall compared to the average, and midcoast Maine faced drought conditions during the sampling period (Epstein 2016). Drought conditions limit freshwater input which can change chemical, physical, and biological estuarine conditions (NOAA 2004). During drought periods, estuaries often become less turbid. During the 2016 drought, however, the DRE was more turbid, which is likely due to increased light absorbing agents, such as CDOM. CDOM can increase due to algal blooms and acid rain (Cory *et al*. 2015). Importantly, the data points are temporally sparse, and while the DRE may have been generally more clear in 2016, the estuary was more turbid during the sampling period.

During non-drought years (e.g. 2017), turbidity in the DRE is likely caused by tidal mixing (McAlice 1977). In 2017, the DRE had fewer light attenuating agents, indicating that turbidity in the DRE is driven by tidal mixing not from sediment input from watersheds. The DRE has muddy sediments which may be suspended more easily than other estuarine substrates (McAlice 1977).

Although the concentration of light attenuating agents varies from 2016 to 2017, the euphotic zone extends deeper than the benthos (Tables 1 and 2). Consequently, optimal microphytobenthos habitat was determined using the half saturation constant, $I=90\mu Em^{-2}s^{-1}$. In 2016 and 2017 in the lower DRE, for example, even though the euphotic zone reached the benthos, the region is classified as sub-optimal habitat because $I<90\mu Em^{-2}s^{-1}$ (Figs. 17 and 18).

Bottom-weighted residual profiles emphasize irradiance at the benthos. Discrepancies between bottom-weighted and non-weighted residuals can be attributed to a non-perfect fit between insolation data and the model. Optimal light resources ($I>90\mu Em^{-2}s^{-1}$) for microphytobenthos primary production are available along the edges of the DRE, and above 43.91ºN (Figs. 17 and 18). Although sub-optimal light conditions ($I<90\mu Em^{-2}s^{-1}$) fall south of 43.91ºN, microphytobenthos can still photosynthesize in these regions because $I=90\mu Em^{-2}s^{-1}$ is only the half saturation value.

Implications for Microphytobenthos in the Damariscotta River Estuary

The contribution of benthic production to total marine primary production is unknown because the surface area where benthic production can occur is overwhelmingly large and their benthic light fields remain largely unstudied (Gattuso *et al*. 2006). Predicting the spatial distribution of microphytobenthos helps determine the most productive regions of the DRE. Microphytobenthos mats are ecologically important in intertidal and subtidal zones because they are rich in nutritional value for herbivorous invertebrates (Hecky and Hesslein 1995). Highly productive regions can potentially support more biomass for higher trophic levels, making the head of the DRE an optimal location for other organisms. Furthermore, microphytobenthos productivity rates have a positive relationship with nutrient cycling rates. In highly productive regions, the rate of nutrient cycling may be greater (Cadée and Hegemann 1974). Finally, the majority of the aquaculture farms are located in optimal habitat regions, and there may be implications for bivalve aquaculture on microphytobenthos primary production and nitrate cycling.

Nitrate fluctuates seasonally along the DRE. Nitrate concentrations peak during the winter, but rapidly decline first during the spring phytoplankton bloom, and again during the midsummer bloom. Nitrate concentrations remain low until they increase during the autumn and winter (McAlice 1977).

Not only does nitrate vary seasonally along the DRE, it also varies spatially. Even in optimal habitats, microphytobenthos are not homogenously present, and nitrate concentrations are not equivalent. In Lowes Cove, for example, microphytobenthos mats are largely absent in the intertidal zone; even when they are present, intracellular nitrate concentrations are very low (Jeremy Rich, personal communication, 21 November 2017).

Microphytobenthos may be absent in intertidal regions due to increased suspension from wave action, predation, or UV exposure. During tidal emersion, individuals may be visually absent following vertical migration into the sediment. Calculating the rate of nitrogen cycling would help elucidate where the majority of the nitrogen is sequestered in the DRE, and thus spatially determine the most productive regions.

Nitrate is especially important for aquaculture farms, as their prerogative is to quickly and efficiently cultivate individuals. Bivalve aquaculture is primarily located at the head of the DRE (DMR Aquaculture Division), and has a positive relationship to microphytobenthos communities. *Crassostrea virginica*, the eastern oyster, (Gmelin 1791) is one of the extensively cultured species in the DRE. Microphytobenthos communities have maximal biomass at the head of the DRE, and are a natural food source for *C. virginia*. In return, *C. virginia* filter particles small than 5μm, and deliver feces, biodeposits (aggregates composed of rejected particulate organic material), and pseudofeces (particles held together by mucus) to the benthos. *C. virginica* effectively reduce light attenuating agents in the water column and deliver inorganic nitrogen and phosphorus to the benthos, stimulating microphytobenthos primary production (Newell and Langdon 1996; Newell et al 2005; Rafaelli *et al*. 1998; Sonchu et al. 2001; Testa et al. 2016; zu Ermgassen and Spalding 2013).

Improvements and Considerations

The model uses PAR to calculate K_d along the benthos of the DRE, which generates optimal light fields that can predict viable microphytobenthos habitat. Including additional variables would transform the basic model into a comprehensive depiction of light fields in the DRE. Incorporating absorbing substances would help stabilize the relationship between experimental and model K_d values. Model K_{dw} residuals are influenced by physical properties of distant water layers, such as turbidity at Glidden Ledges in 2016 (Figure 6). Although the upper 18m fit the semilog line, the slope is impacted by turbid benthic waters (Fig. 6). Incorporating error (+/- 10%) in K_{dw} measurements would help reduce variance.

Importantly, the spectral quality of transmitted light is directly related to depth, and accounting for low-quality light at the benthos would most accurately predict benthic primary production. Light at the benthos is also influenced by reflection; blue and green light can reflect off the benthos. Once reflected, it can travel back toward the surface, or it can be scattered back down to microphytobenthos and increase ambient light levels (Harris and Baker 2014). Benthic reflectance may account for increased benthic K_d residuals (Figs. 3, 9 – 12). Although bottom-weighted K_d profiles emphasize light resources at the benthos, they fail to take reflective processes into account.

Light patterns not only vary spatially, but also seasonally and yearly. Data was collected on September 21st in 2016, and September 27th in 2017. The equinox fell on September 22nd in 2016 and in 2017, so more sunlight compared to the rest of the year was present during the sampling period. Data is comparable from 2016 to 2017, but may not be indicative of sunlight reaching the benthos during the remainder of the year.

Sampling at the same time each month under similar atmospheric conditions would provide a more accurate description of light reaching the benthos year round. Furthermore, gathering data from multiple years helps normalize weather events that influence light transmission, such as drought, temperature, and cloud cover.

Besides light, benthic topography and substrate impact microphytobenthos habitat. Strong currents and tides not only suspend microphytobenthos, but also cause sediment suspension that decreases light quality. Topographically, microphytobenthos communities have higher biomass in flat, muddy environments, compared to sloping, sandy environments. Geographically examining current velocity, tidal cycles, substrate and topography would help spatially predict sustainable microphytobenthos communities.

In conclusion, microphytobenthos communities are an integral component of benthic marine ecosystems. Although this model is rudimentary, it is the first benthic light field map of the DRE. Subsequent comprehensive models should include components of turbidity, light attenuating agents, benthic light reflection, benthic spectral quality, the presence/absence of accessory pigments in microphytobenthos, current velocity, substrate, and topography. As primary producers, microphytobenthos are an integral ecological component of estuarine systems. Understanding viable microphytobenthos habitat in the DRE helps us to discover where nitrogen is being spatially sequestered, and potential locations for the most productive aquaculture farms.

LITERATURE CITED

Abe, H., N. Hasegawa, S. Yoon, M. J. Kishi. "Evaluation of Manila clam (*Ruditapes philippinarum*) growth and microphytobenthos resuspension in a subarctic lagoon in Japan." *Hydrobiologia*., vol. 758, no. 1, 2015, pp. 87-98.

Aberle-Malzahn, N. "The Microphytobenthos and Its Role in Aquatic Food Webs." *Doctoral Dissertation for Christian-Albrechts-University*, 2004, pp. 1–103.

Admiraal, W. "Tolerance of estuarine benthic diatoms to high concentrations of ammonia, nitrite ion, nitrate ion and orthophosphate*." Marine Biology*, vol. 43, 1977, pp. 307-315.

Admiraal, W. "The ecology of estuarine sediment inhabiting diatoms*." Progress in Phycological Research*, vol. 3, 1984, pp. 269.

Ashworth, J., S. Coesel, A. Lee, E. V. Armbrust, M. V. Orellana, N. S. Baliga. "Genome-wide diel growth state transitions in the diatom Thalassiosira pseudonana." *National Academy of Sciences*, vol. 110, no. 18, 2013, pp. 7518-7523.

Asmus R. M. and H. Asmus. "Mussel beds: limiting or promoting phytoplankton?" *Jour. Exp. Mar. Biol. Ecol.*, vol. 148, 1991, pp. 215-232.

Baker, E. T., and J. W. Lavelle. "The effect of particle size on the light attenuation coefficient of natural suspensions." *Journal of Geophysical Research*, vol. 89, no. C5, 1984, pp. 8197-8203.

Blanchard, G. H., J. M. Guarini, P. Richard, P. Gros, F. Mornet. "Quantifying the short-term temperature effect on light-saturated photosynthesis of intertidal microphytobenthos." *Mar. Ecol. Prog. Ser*., vol. 134, 1996, pp. 309–313.

Brotas, V. and F. Catarino. "Microphytobenthos primary production of Tagus estuary intertidal flats (Portugal)." *Neth. Jour. Aquat. Ecol*., vol. 29, 1995, pp. 333–339

Cadée, G. C., J. Hegeman. "Primary production of the benthic microflora living on tidal

flats in the Dutch Wadden Sea*." Netherlands Journal of Sea Research*, vol. 8, 1974, pp. 260-291.

Cahoon, L. B., Beretich, G. R., J., Thomas, C. J., and McDonald, A. M. "Benthic microalgal production at Stellwagen Bank, Massachusetts Bay, USA." *Mar. Ecol. Prog. Ser.,* vol. 102, 1993, pp. 179–185.

Cerco, C. F., and S. P. Seitzinger. "Measured and Modeled Effects of Benthic Algae on Eutrophication in Indian River-Rehoboth Bay, Delaware." *Estuaries*, vol. 20, Mar. 1997, pp. 231–248.

Cook, P. L. M., B. Veuger, S. Böer, J. L. Middleburg. "Effect of nutrient availability on carbon and nitrogen incorporation and flows through benthic algae and bacteria in near-shore sandy sediments." *Aquat. Microb. Ecol.*, vol. 49, no. 2, 2007, pp. 165-180.

Cheney, D. "Assessment of Environmental Impacts of Oyster Aquaculture in New England Waters: Objective 3. Assess benthic infaunal, epifaunal, meiofaunal and macrofaunal impacts." *NRAC Oyster Project*, 30. Jun. 2012, pp. 1-21.

Coljin, F. "Light absorption in the waters of the Ems-Dollard Estuary and its consequences for the growth of phytoplankton and microphytobenthos." *Netherlands Journal of Sea Research*, vol. 15, no. 2, 1982, pp. 196-216.

Coljin, F. and V. N. de Jonge. "Primary production of mircophytobenthos in the Ems-Dollard Estuary." *Mar. Ecol. Prog. Ser.*, vol. 14, 2 Jan. 1984, pp. 185-196.

Cory, R. M., K. H. Harrold, B. T. Neilson, G. W. Kling. "Controls on dissolved organic matter (DOM) degradation in a headwater stream: the influence of photochemical and hydrological conditions in determining light-limitation or substrate-limitation of photo-degradation." *Biogeosciences*, vol. 12, 2015, pp. 6669-6685.

de Jong, L. and W. Admiraal. "Copetition between three estuarine benthic diatom species in mixed cultures." *Mar. Ecol. Prog. Ser.*, vol. 18, 15 Aug. 1984, pp. 269-275.

de Jonge, V. N., F. Colijn. "Dynamics of microphytobenthos biomass in the Ems estuary." *Mar. Ecol. Prog. Ser.*, vol. 104, 1994, pp. 185-196.

Delgado, M. “Abundance and distribution of microphytobenthos in the bays of Ebro Delta (Spain*).” Estuarine, Coastal and Shelf Science*, vol. 29, 1989, pp. 183-194.

Delgado, M., V. N. de Jonge, H. Peletier. “Experiments on resuspension of natural microphytobenthos populations.” *Mar. Bio.*, vol. 108, 1991, pp. 321-328.

Department of Marine Resources Aquaculture Division. “Map of Aquaculture Leases with Shellfish Growing Area Classification Information and Lease Decision Documents.” *Maine Department of Marine Resources*, 2017.

Epstein, D. *“In spite of recent rain, drought – uncommon for Maine – continues.”* The Portland Press Herald / Maine Sunday Telegram, 2016. Available from http://www.pressherald.com/2016/10/18/spite-recent-rain-drought-continues/.

Falciatore, A. and C. Bowler. “The Evolution and Function of Blue and Red Light Receptors.” *Elsevier*, vol. 68, 2005, pp. 317-350.

Gattuso, J. P., Gentili, B., Duarte, C. M., Kleypas, J. A., Middelburg, J. J., and Antoine, D. *“Light availability in the coastal ocean: impact on the distribution of benthic photosynthetic organisms and their contribution to primary production.”* Bio geo sci, vol. 3, 2006, pp. 489-513.

“GNIS Detail - Damariscotta River.” *Geographic Names Information System (GNIS)*, United States Geological Survey.

Govindjee. “A Role for a Light-Harvesting Antenna Complex of Photosystem II in Photoprotection.” *The Plant Cell*, vol. 14, no. 8, 2002, pp. 1663–1668.

Harris, Peter T., and Elaine K. Baker. *Seafloor Geomorphology as Benthic Habitat: GeoHAB Atlas of Seafloor Geomorphic Features and Benthic Habitats*. Elsevier Science, 2014.

Hayward, J. *New England Gazetteer*. Nabu Press, 2010.

Hecky, R. E. and R. H. Hesslein. "Contributions of benthic algae to lake food webs as revealed by stable isotope analysis." *Journal of the North American Benthological Society*, vol. 14, 1995, pp. 631-653.

Henriksen, K., J. Hansen, T. H. Blackburn. "The influence of benthic infauna on exchange rates of inorganic nitrogen between sediment and water." *Ophelia*, vol. 1, 1980, pp. 249-256.

Hopkins, J. "A study of the diatoms of the Ouse estuary, Sussex. I. The movement of the mud-flat diatoms in response to some chemical and physical changes." *Journal of the Marine Biological Association of the United Kingdom*, vol. 43, 1963, pp. 653-663.

Joergensen, B. B., N. P. Revsbech, Y. Cohen. "Photosynthesis and structure of benthic microbial mats: Microelectrode and SEM studies of four cyanobacterial communities." *Limnology & Oceanography*, vol. 28, 1983, pp. 1075-1093.

Kaspar, H. F., P. A. Gillespie, I. C. Boyer, A. L. MacKenzie. "Effects of mussel aquaculture on the nitrogen cycle and benthic communities in Kenepuru South, Marlborough Sounds, New Zealand." *Mar. Biol.*, vol. 85, 1985, pp. 127-136.

Kromkamp, J., C. Barranguet, J. Peene. "Determination of microphytobenthos PSII quantum efficiency and photosynthetic activity by means of variable chlorophyll fluorescence." Mar. Ecol. Prog. Ser., vol. 162, 1998, pp. 45–55.

Kemp, W. M., W. R. Boynton, J. E. Adolf, D. F. Boesch, W. C. Boicourt, G. Brush, J. C. Cornwell, T. R. Fisher, P. M. Glibert, J. D. Hagy, L. W. Harding, E. D. Houde, D. G. Kimmel, W. D. Miller, R. I. E. Newell, M. R. Roman, E. M. Smith, J. C. Stevenson. "Eutrophication of Chesapeake Bay: historical trends and ecological interactions." *Mar. Ecol. Prog. Ser*, vol. 303, 21 Nov. 2005, pp. 1-29.

Kirk, J. T. O. "Light and Photosynthesis in Aquatic Ecosystems." 2nd ed., *Cambridge University Press*, 1994, p. 509.

Kirk, J. T. O. "Use of a quanta meter to measure attenuation and underwater reflectance of photosynthetically active radiation in some inland and coastal Southeastern Australian waters." *Australian Journal of Marine and Freshwater Resources*, vol. 28. 1977, pp. 9-21.

Liu, W. “Water column light attenuation estimation to simulate phytoplankton population in tidal estuary.” *Environ. Geo.*, vol. 49, no. 1, 2005, pp. 280-292.

MacIntyre, I. G., L. Prufert-Bebout, P. R. Reid. “The role of endolithic cyanobacteria in the formation of lithified laminae in Bahamian stromatolites.” *Journal of the International Association of Sedimentologists,* vol. 46, no. 5, Oct. 2000, pp. 915-921.

McAlice, B. J. “A Preliminary Oceanographic Survey of the Damariscotta River Estuary, Lincoln County, Maine.” *Maine Sea Grant Technical Report*, 1977, pp. 1-63.

Middleburg, J. J., C. Barranguet, H. T. S. Boschker, P. M. J. Herman, T. Moens, C. H. R. Heip. “The fate of intertidal microphytobenthos carbon: an in situ 13C-labelling study.” *Limnol. Oceanogr.*, vol. 45, 2000, pp. 1224–1234.

Mitbavkar, S. and A. C. Anil. “Diatoms of the microphytobenthic community: population structure in a tropical intertidal sand flat*.” Marine Biology*, vol. 140, 2002, pp. 41-57.

Morel, A. “Optical Modeling of the Upper Ocean in Relation to Its Biogenous Matter Content (Case I Waters).” *Journal of Geophysical Research*, vol. 93, no. C9, 15 Sep. 1988, pp. 10,749-10,768.

Müller, P., L. Xiao-Ping, K. N. Krishna. “Non-Photochemical Quenching. A Response to Excess Light Energy.” *American Society of Plant Physiologists*, vol. 125, no. 4, 2001, pp. 1558-1566.

National Oceanic and Atmospheric Administration (NOAA). “What Is an Estuary?” *NOAA's National Ocean Service*, United States Department of Commerce, 8 Oct. 2008.

Netto, A. T., E. Campostrini, J. Goncalves de Oliveira, R. E. Bressan-Smith. “Photosynthetic pigments, nitrogen, chlorophyll a fluorescence and SPAD-502 readings in coffee leaves.” *Scientia Horticulturae*, vol. 104, no. 2, 2005, pp. 199-209.

Newell, R. I. E. and C. J. Langdon. "Mechanisms and physiology of larval and adult feeding (Chapter 5). In: Kennedy VS, Newell RIE, Eble A (eds) The eastern oyster, Crassostrea virginica." *Maryland Sea Grant*, 1996.

Newel, R. I. E., J. Cornwell, M. S. Owens. "Influence of simulated bivalve biodeposition and microphytobenthos on sediment nitrogen dynamics: a laboratory study." *Limnol. Oceanogr*., vol. 47, 2002, pp. 1367–1379.

Newel, R. I. E., T. R. Fisher, R. R. Holyoke, J. C. Cornwell. "Influence of eastern oysters on N and P regeneration in Chesapeake Bay, USA." *Springer*, 2005, pp. 93–12.

Nozaki, K., D. Khadbaatar, A. Tetsuji, G. Naoshige, M. Osamu. "Development of filamentous green algae in the benthic algal community in a littoral sand-beach zone of Lake Biwa." *Limnology*, vol. 4, 2003, pp. 161-165.

Orth, R. J., and K. A. Moore. "Chesapeake Bay: An Unprecedented Decline in Submerged Aquatic Vegetation." *Science*, vol. 222, no. 4619, 1983, pp. 51-53.

Paterson, D. M. "Microbiological mediation of sediment structure and behaviour." *Microbial mats. NATO ASI series*, vol. G35, 1994, pp. 97–109.

Perkins, R. G., G. J. C. Underwood, V. Brotas, G. C. Snow, B. Jesus, L. Ribeiro**.** "Responses of microphytobenthos to light: primary production and carbohydrate allocation over an emersion period." *Mar. Ecol. Prog. Ser.*, vol. 223, 28 Nov. 2001, pp. 101-112.

Pinckney, J. and R. G. Zingmark. "Effects of tidal stage and sun angles on intertidal benthic microalgal productivity." *Mar. Ecol. Prog. Ser.*, vol. 76, no. 1, 18 Sept. 1991, pp. 81-89.

Postma, H. "Sediment transport and sedimentation in the estuarine environment." *Estuaries. Am. Assoc. Adv. Sci. Washington D. C.*, 1967, pp. 158-179.

Potter, I. C., D. Cannon, J. W. Moore. "The ecology of algae in the Moruya River Australia." *Hydrobiologia*, vol. 47, 1975, pp. 415-430.

Pullin, M. J. and S. E. Cabaniss. “The effects of pH, ionic strength, and iron–fulvic acid interactions on the kinetics of non-photochemical iron transformations. I. Iron(II) and iron(III) colloid formation.” *Geochimica et Cosmochimica Acta*, vol. 67, no. 21, 2003, pp. 4067-4077

Rafaelli, D. G., J. A. Raven, L. J. Poole. “Ecological impact of green macroalgal blooms.” *Oceanogr. Mar. Biol. Annu. Rev*., vol. 36, 1998, pp. 97 – 125.

Richardson, T. L., J. J. Cullen, D. E. Kelley, M. R. Lewis. “Potential contributions of vertically migrating *Rhizosolenia* to nutrient cycling and new production in the open ocean.” *J. Plankton Res.*, vol. 20, 1998, pp. 219-241.

Riisgaard, H.U. “Efficiency of particle retention and filtration rate in 6 species of Northeast American bivalves.” *Mar. Ecol. Prog. Ser*., vol. 45, 1988, pp. 217–223.

Ryther, J. H., and Menzel, D. W. “Light Adaptation by Marine Phytoplankton.” *Limnology and Oceanography*., vol. 4, 1959, pp. 492-497.

Seitzinger, S. P. “Denitrification in freshwater and coastal marine ecosystems: ecological and geochemical signififcance.” *Limnol. Oceanogr.*, vol. 33, 1988, pp. 702-724.

Souchu, P., A. Vaquer, Y. Collos, S. Landrein, J. M. Deslous-Paoli, B. Bibern. “Influence of shellfish farming activities on the biogeochemical composition of the water column in Thau lagoon.” *Mar. Ecol. Prog. Ser*., vol. 218, 2001, pp. 141–152.

Sundbäck, K, A. Miles, E. Göransson. “Nitrogen fluxes, denitrification and the role of mircophytobenthos in microtidal shallow-water sediments: an annual study.” *Mar. Ecol. Prog. Ser.*, vol. 200, 2000, pp. 59-76.

Taylor, M. R., E. J. Simon, J. Dickey, K. A. Hogan, J. B. Reece, N. A. Campbell. *Campbell Biology: Concepts & Connections*. 9th ed., Pearson Education, Inc., 2010.

Testa, J. M., D. C. Brady, J. C. Cornwell, M. S. Owens, L. P. Sanford, C. R. Newell, S. E. Suttles, R. E. Newell. “Modeling the impact of floating oyster

(Crassostrea virginica) aquaculture on sediment−water nutrient and oxygen fluxes." *Aquacult. Environ. Interact.*, vol. 7, 21 Oct. 2016, pp. 205-222.

Tyler, J. E. "Report on the second meeting of the Joint Group of experts of photosynthetic radiant energy." *UNESCO Tech. Pap. Mar. Sci.*, vol. 2, 1966, pp. 1-11.

Underwood, G. J. C. and D. J. Smith. "Predicting epipelic diatom exopolymer concentrations in intertidal sediments from sediment chl a." *Microb. Ecol*., vol. 35, 1998, pp. 116–125.

Underwood, G. J. C. and J. Kromkamp. "Primary production by phytoplankton and microphytobenthos in estuaries." *Adv. Ecol. Res*., vol. 29, 1999, pp. 93–153.

US Department of Commerce, National Oceanic and Atmospheric Administration. "NOAA's National Ocean Service Education: Estuaries." *NOAA's National Ocean Service*, 19 Dec. 2004. Available from: oceanservice.noaa.gov/education /kits/estuaries/media/supp_estuar10b_depth.html.

Yallop, M. L., W. B. De, D. M. Paterson, L. J. Stal. "Comparative structure, primary production and biogenic stabilization of cohesive and non-cohesive marine sediments inhabited by microphytobenthos." *Estuarine, Coastal and Shelf Science*, vol. 39, 1994, pp. 565-582.

zu Ermhassen, P. S. E. and M. D. Spalding. "Quantifying the Loss of a Marine Ecosystem Service: Filtration by the Eastern Oyster in US Estuaries." *Estuaries and Coasts*., vol. 36, 2013, pp. 36-43.

Zumft, W. "Cell biology and molecular basis of denitrification." *Microbio. Mol. Biol. Rev.*, vol. 61, 1997, pp. 533-616.

APPENDIX

Table 1: Bottom depth, $Z_{1\%}$, experimental K_d, model K_d, and optimal light level depth in the Damariscotta River Estuary on 21 September 2016.

Station	Bottom Depth (m)	$Z_{1\%}$ (m)	Experimental K_d	Model K_d	Depth (m) where irradiance < $90\mu Em^{-2}s^{-1}$
6 (Head)	4.5	9.588438969	0.480	0.456	--
5	3.5	9.790855261	0.470	0.469	--
4	12	16.29924955	0.283	0.260	> 23.3599
3 (Glidden Ledges)	21.6	14.68257696	0.314	0.332	> 23.6578
2	20.5	38.05711265	0.121	0.194	> 23.9419
1 (Mouth)	34.7	40.02109592	0.115	0.112	> 23.9901

Table 2: Bottom depth, $Z_{1\%}$, experimental K_d, model K_d, and optimal light level depth in the Damariscotta River Estuary on 21 September 2016.

Station	Bottom Depth (m)	$Z_{1\%}$ (m)	Experimental K_d	Model K_d	Depth (m) where irradiance < $90\mu Em^{-2}s^{-1}$
6 (Head)	5.25	22.68556742	0.203	0.217	--
5	7	18.2022537	0.253	0.234	--
4	12.25	21.51948685	0.215	0.276	> 10
3 (Glidden Ledges)	16.75	22.57436366	0.204	0.204	> 10
2	22.056	28.78231366	0.160	0.168	> 11.508
1 (Mouth)	28	33.61438092	0.137	0.150	> 12.75

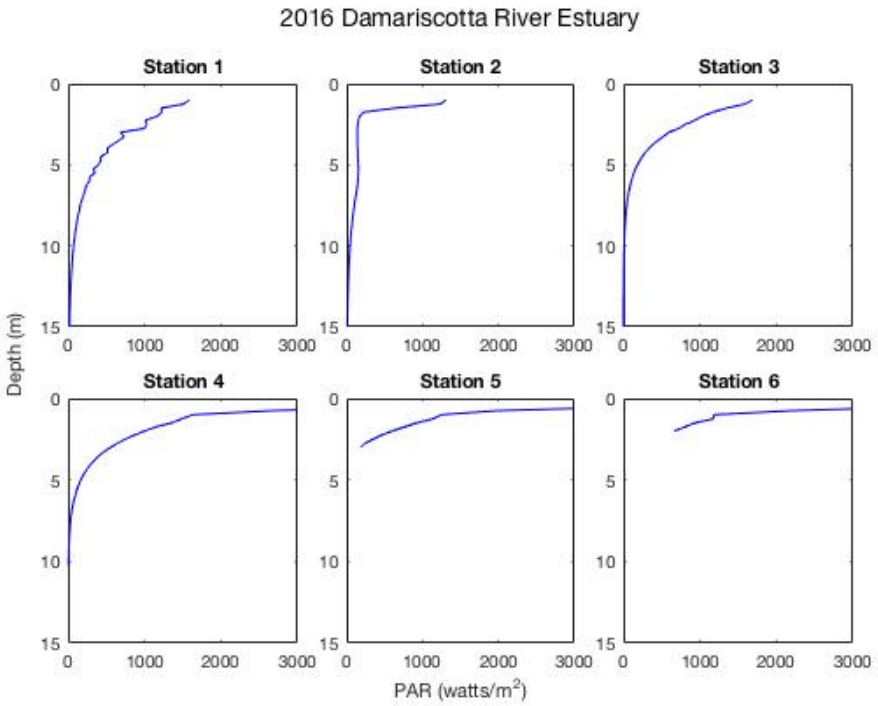

Figure 1: 2016 Damariscotta River Estuary PAR attenuation (watts/m^2) versus depth (m). PAR is inversely proportional to depth.

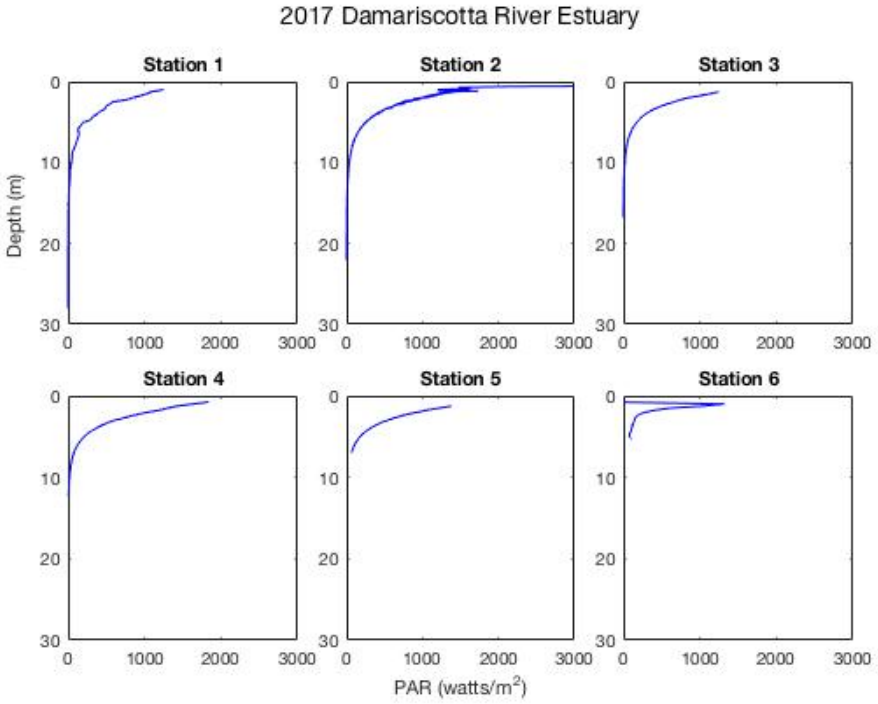

Figure 2: 2017 Damariscotta River Estuary PAR attenuation (watts/m^2) versus depth (m). PAR is inversely proportional to depth.

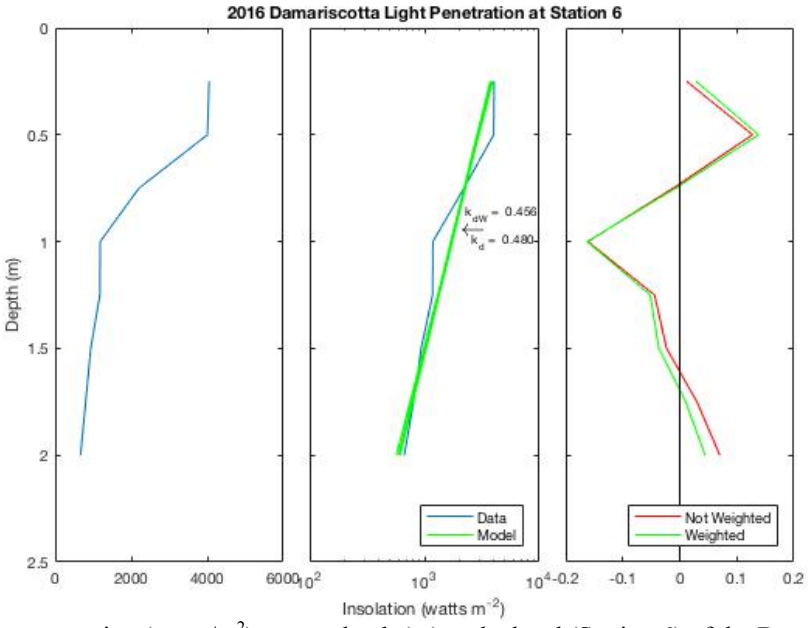

Figure 3: Light penetration (watts/m^2) versus depth (m) at the head (Station 6) of the Damariscotta River Estuary on 21 September 2016. GPS coordinates: 44.032ºN, 69.535ºW. Plots from left to right: irradiance reaching the benthos; blue and green lines represent data and model respectively; red and green lines represent non-weighted and weighed residuals respectively.

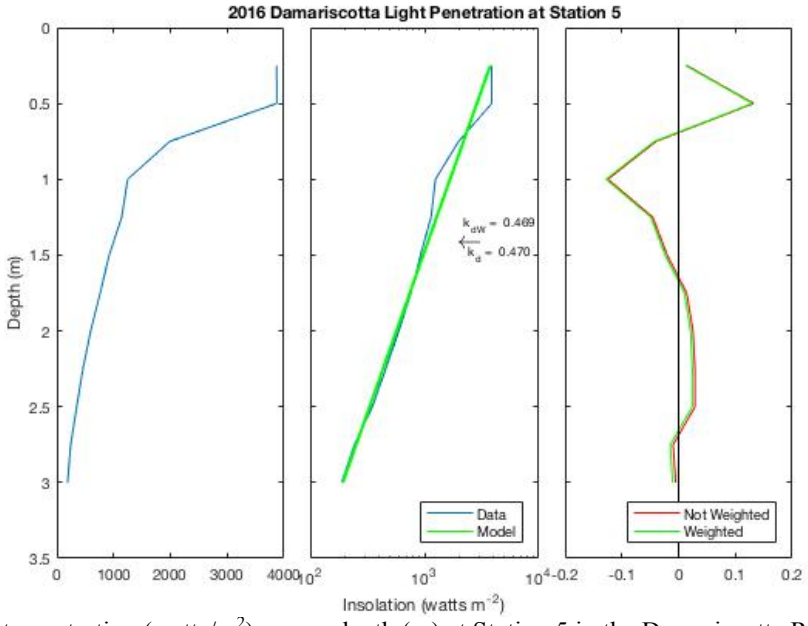

Figure 4: Light penetration (watts/m^2) versus depth (m) at Station 5 in the Damariscotta River Estuary on 21 September 2016. GPS coordinates: 44.999ºN, 69.541ºW. Plots from left to right: irradiance reaching the benthos; blue and green lines represent data and model respectively; red and green lines represent non-weighted and weighed residuals respectively.

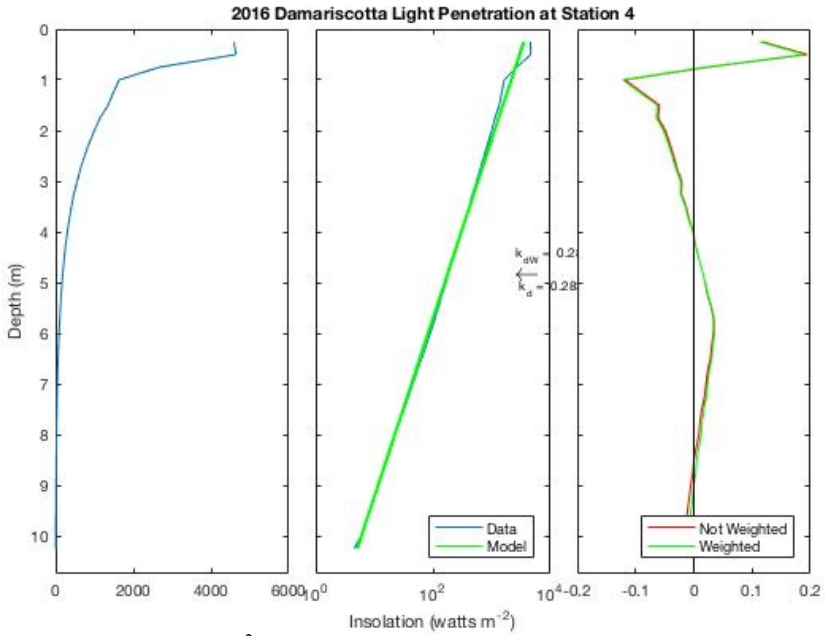

Figure 5: Light penetration (watts/m^2) versus depth (m) at Station 4 in the Damariscotta River Estuary on 21 September 2016. GPS coordinates: 44.936ºN, 69.582ºW. Plots from left to right: irradiance reaching the benthos; blue and green lines represent data and model respectively; red and green lines represent non-weighted and weighed residuals respectively.

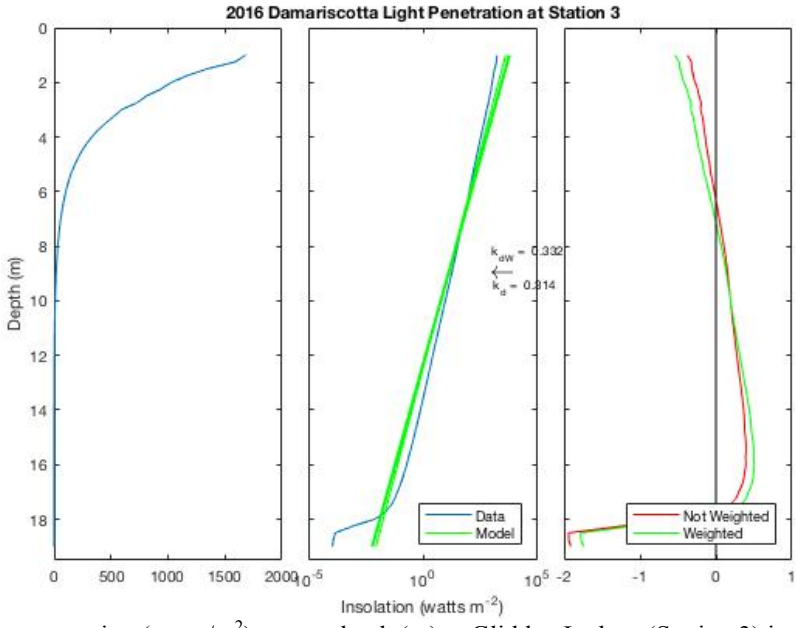

Figure 6: Light penetration (watts/m^2) versus depth (m) at Glidden Ledges (Station 3) in the Damariscotta River Estuary on 21 September 2016. GPS coordinates: 44.91ºN, 69.571ºW. Plots from left to right: irradiance reaching the benthos; blue and green lines represent data and model respectively; red and green lines represent non-weighted and weighed residuals respectively.

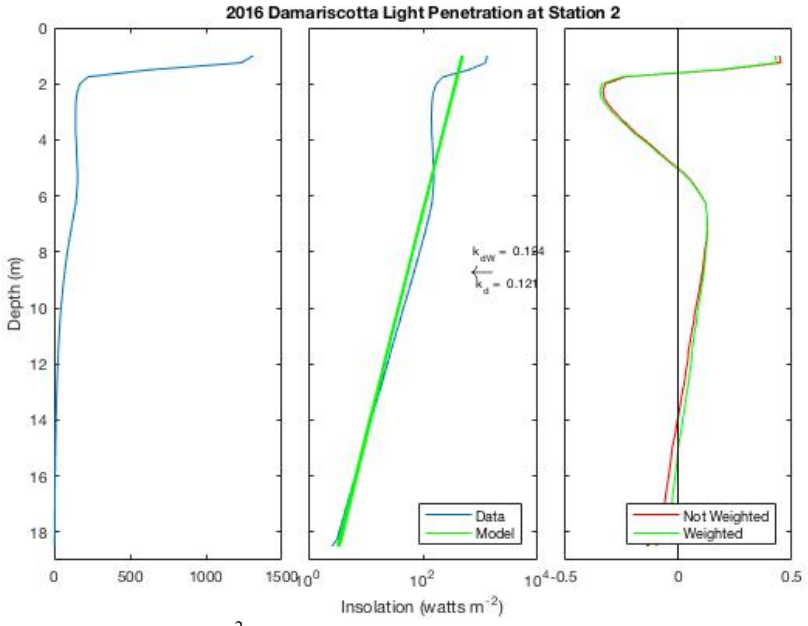

Figure 7: Light penetration (watts/m^2) versus depth (m) at Station 2 in the Damariscotta River Estuary on 21 September 2016. GPS coordinates: 44.872ºN, 69.5786ºW. Plots from left to right: irradiance reaching the benthos; blue and green lines represent data and model respectively; red and green lines represent non-weighted and weighed residuals respectively.

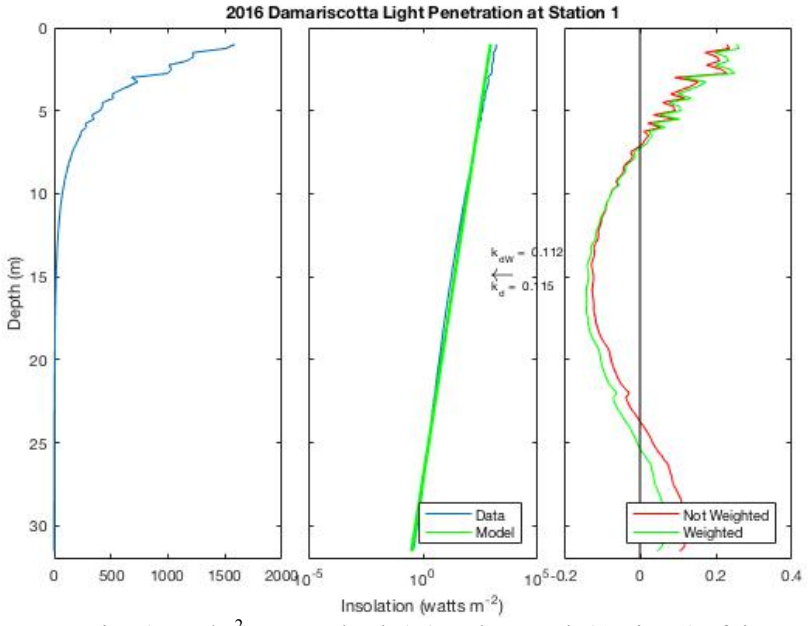

Figure 8: Light penetration (watts/m^2) versus depth (m) at the mouth (Station 1) of the Damariscotta River Estuary on 21 September 2016. GPS coordinates: 44.836ºN, 69.572ºW. Plots from left to right: irradiance reaching the benthos; blue and green lines represent data and model respectively; red and green lines represent non-weighted and weighed residuals respectively.

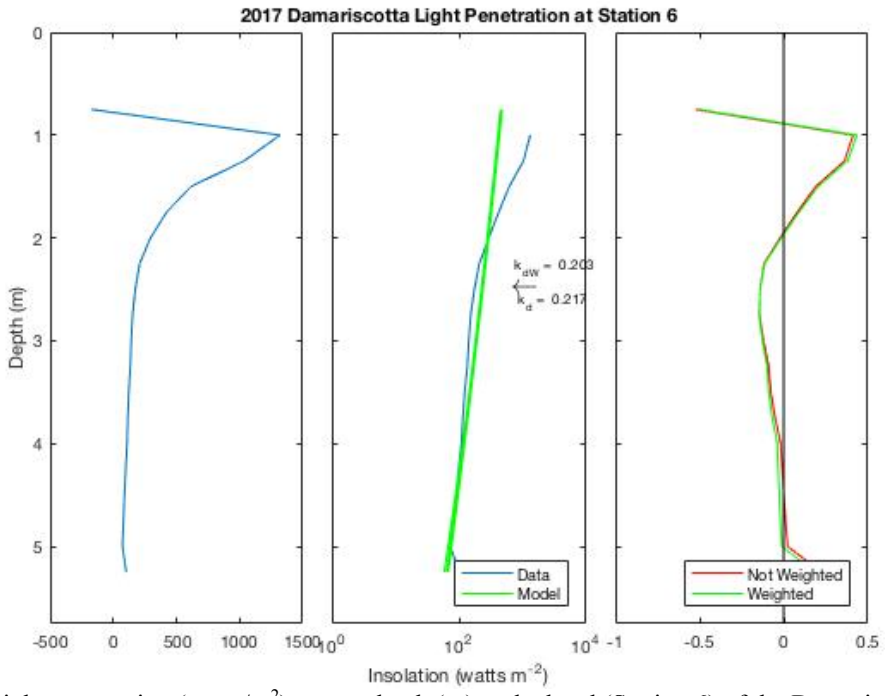

Figure 9: Light penetration (watts/m^2) versus depth (m) at the head (Station 6) of the Damariscotta River Estuary on 27 September 2017. GPS coordinates: 44.8368ºN, 69.572ºW. Plots from left to right: irradiance reaching the benthos; blue and green lines represent data and model respectively; red and green lines represent non-weighted and weighed residuals respectively.

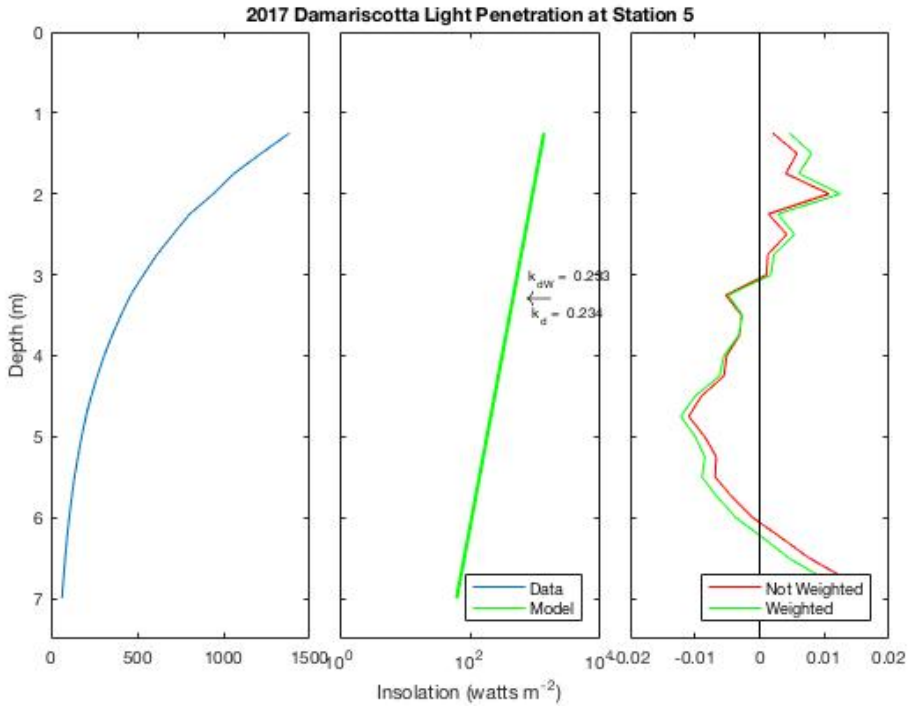

Figure 10: Light penetration (watts/m^2) versus depth (m) at Station 5 of the Damariscotta River Estuary on 27 September 2017. GPS coordinates: 44.877ºN, 69.581ºW. Plots from left to right: irradiance reaching the benthos; blue and green lines represent data and model respectively; red and green lines represent non-weighted and weighed residuals respectively.

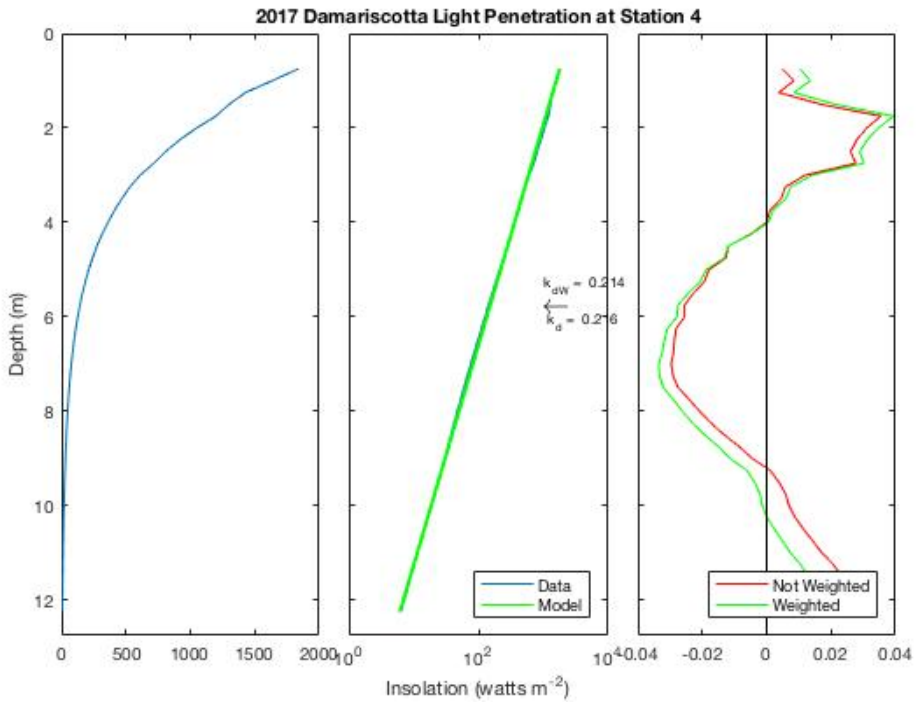

Figure 11: Light penetration (watts/m^2) versus depth (m) at Station 4 of the Damariscotta River Estuary on 27 September 2017. GPS coordinates: 44.913ºN, 69.5721ºW. Plots from left to right: irradiance reaching the benthos; blue and green lines represent data and model respectively; red and green lines represent non-weighted and weighed residuals respectively.

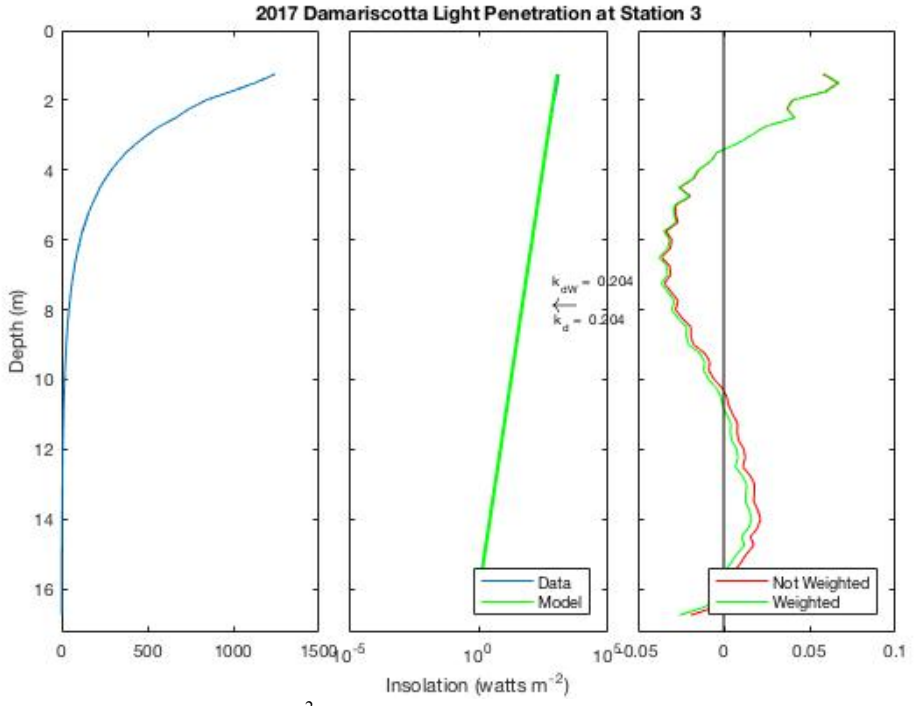

Figure 12: Light penetration (watts/m^2) versus depth (m) at Station 3 of the Damariscotta River Estuary on 27 September 2017. GPS coordinates: 44.9535ºN, 69.583ºW. Plots from left to right: irradiance reaching the benthos; blue and green lines represent data and model respectively; red and green lines represent non-weighted and weighed residuals respectively.

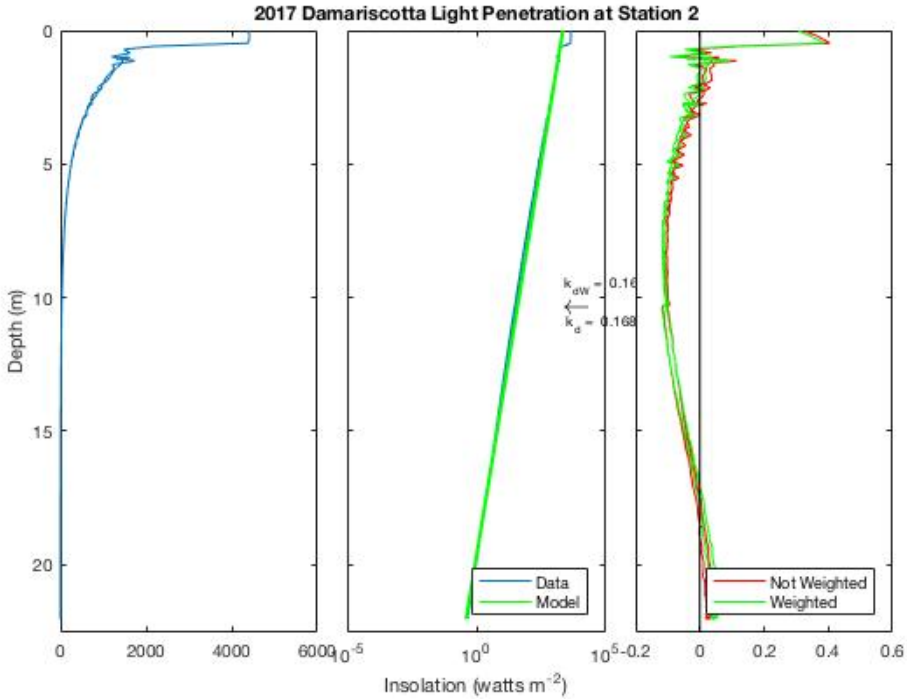

Figure 13: Light penetration (watts/m^2) versus depth (m) at Station 2 of the Damariscotta River Estuary on 27 September 2017. GPS coordinates: 44.978ºN, 69.5615ºW. Plots from left to right: irradiance reaching the benthos; blue and green lines represent data and model respectively; red and green lines represent non-weighted and weighed residuals respectively.

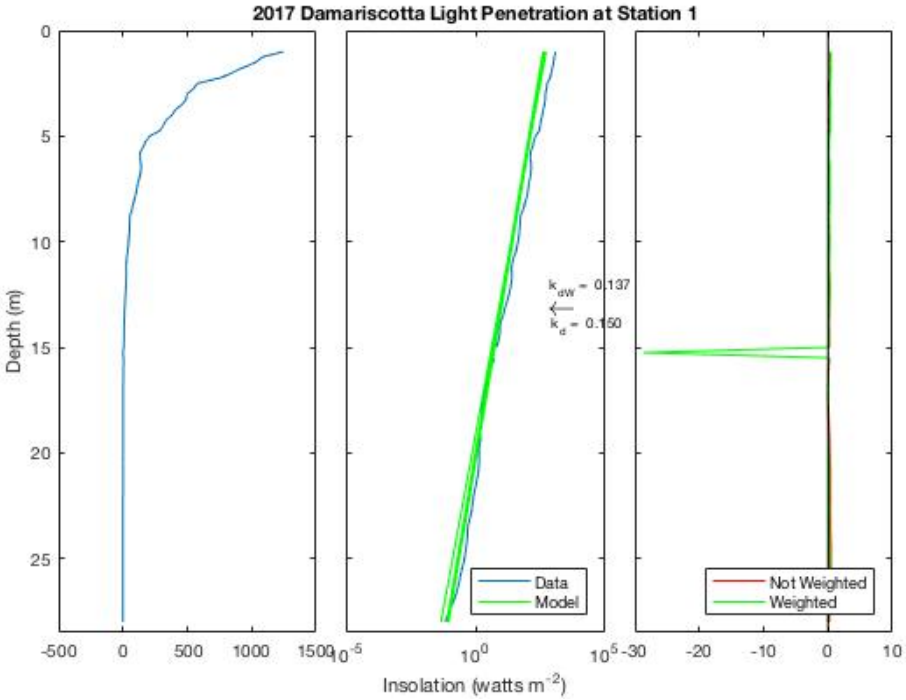

Figure 14: Light penetration (watts/m^2) versus depth (m) at the mouth (Station 1) of the Damariscotta River Estuary on 27 September 2017. GPS coordinates: 44.0315ºN, 69.536ºW. Plots from left to right: irradiance reaching the benthos; blue and green lines represent data and model respectively; red and green lines represent non-weighted and weighed residuals respectively.

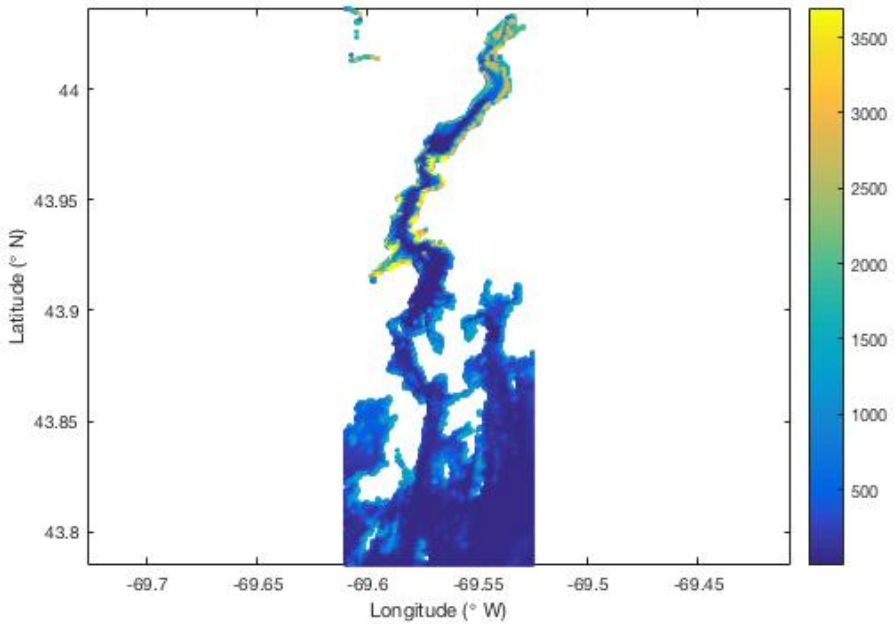

Figure 15: Bathymetric plot of the Damariscotta River Estuary. Color bar represents $\log_{10}$ of irradiance (watts/m^2).

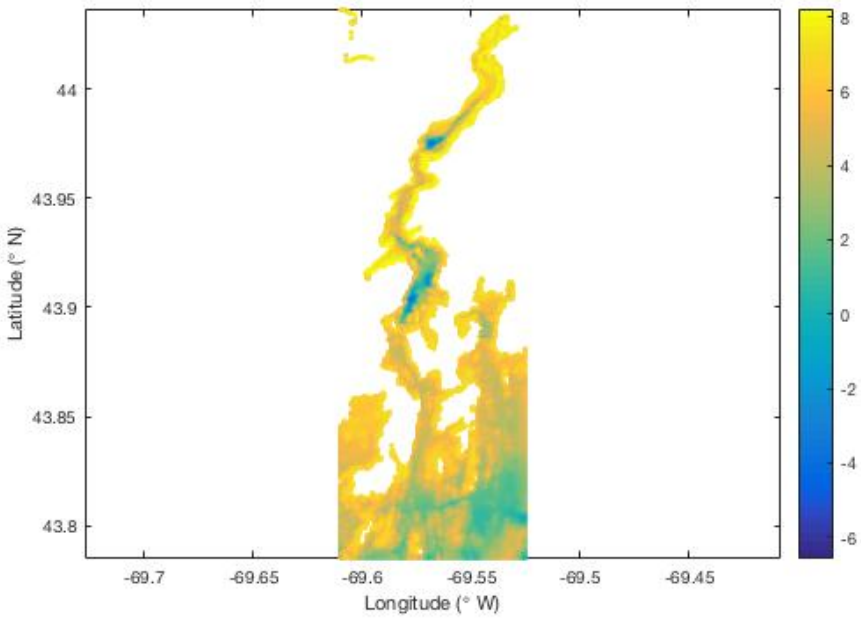

Figure 16: Bathymetric plot of the Damariscotta River Estuary. Color bar represents the natural log of irradiance (watts/m^2).

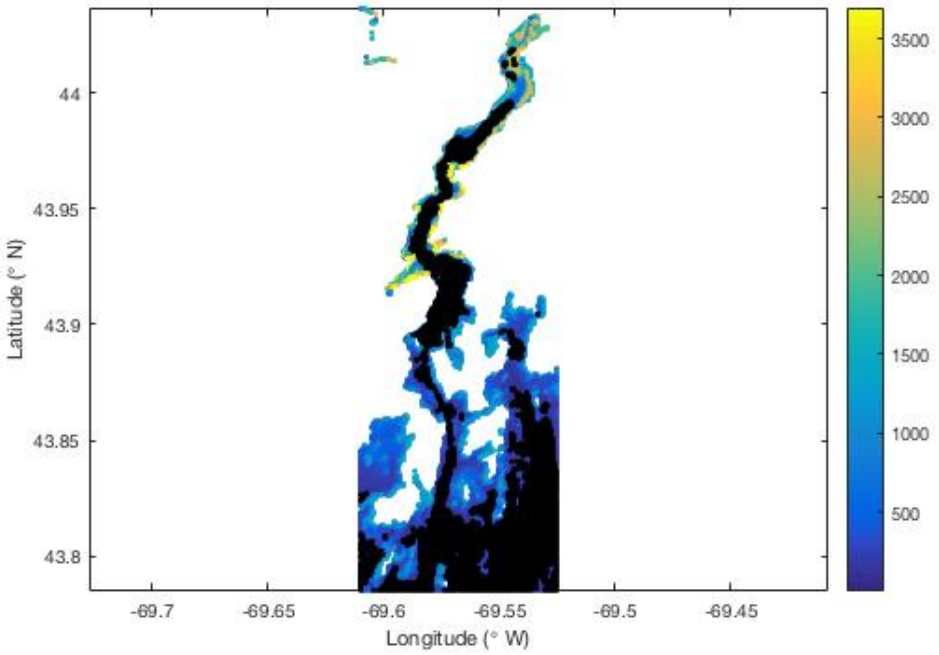

Figure 17: Bathymetric plot of the Damariscotta River Estuary. Color bar represents the $\log_{10}$ of irradiance (watts/m^2). Dark fill corresponds to river area where I<90μE/m^2s on the benthos.

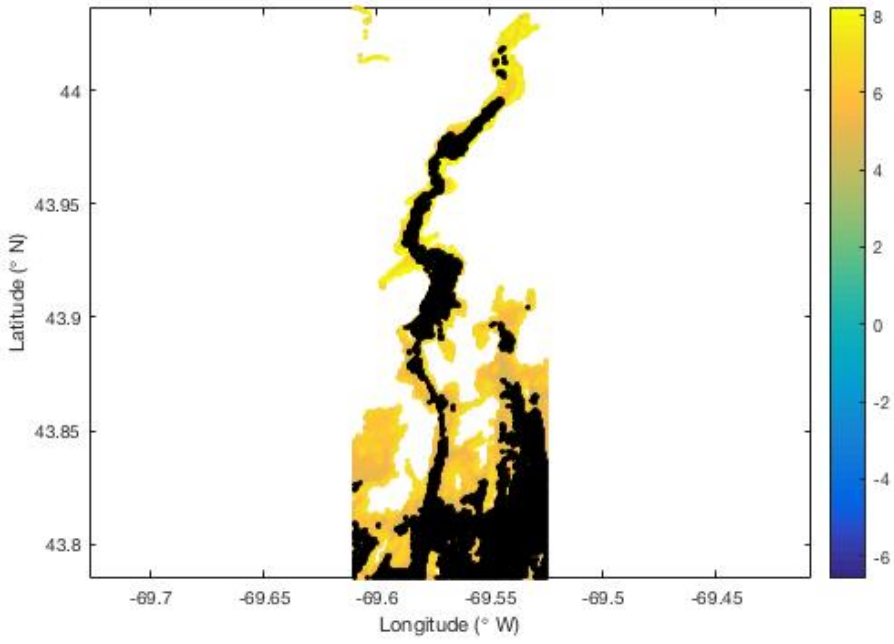

Figure 18: Bathymetric plot of the Damariscotta River Estuary. Color bar represents the natural log of irradiance (watts/m^2). Dark fill corresponds to river area where I<90μE/m^2s on the benthos.

AUTHOR'S BIOGRAPHY

Born in Oriental, North Carolina on January 1st, 1996, Teiga Martin lived in a variety of countries before Maine. In 2014 she graduated from Lincoln Academy High School in Newcastle, Maine. Teiga majors in marine science, with a concentration in biology, and minors in music. During her junior year, Teiga studied at Semester by the Sea at the Darling Marine Center in Walpole, Maine. Following graduation in December 2017, Teiga will teach scientific SCUBA diving in Greece, then will return to the United States to pursue an advanced degree in marine science.